Molecular mechanism of transglutaminase-2 in corneal epithelial migration and adhesion

Louis Tong [a,b,c,d,*], Evelyn Png [a], Hou AiHua [a], Siew Sian Yong [a], Hui Ling Yeo [a], Andri Riau [a], Earnest Mendoz [e], Shyam S. Chaurasia [a,d,e], Chwee Teck Lim [f], Ting Wai Yiu [g], Siiri E. Iismaa [g]

[a] Ocular Surface Research Group, Singapore Eye Research Institute, Singapore 168751, Singapore
[b] Department of Cornea and External Eye Disease, Singapore National Eye Center, 11 Third Hospital Avenue, Singapore 168751, Singapore
[c] Office of Clinical Science, Duke-NUS Graduate Medical School, Singapore
[d] Department of Ophthalmology, Yong Loo Lin School of Medicine, National University of Singapore, Singapore
[e] SRP Neuroscience and Behavioral Disorders, Duke-NUS Graduate Medical School, Singapore
[f] Division of Bioengineering & Department of Mechanical Engineering, National University of Singapore, 9 Engineering Drive 1, Singapore 117576, Singapore
[g] Molecular Cardiology Program, Victor Chang Cardiac Research Institute, 405 Liverpool St., Darlinghurst, NSW 2010 Australia

ARTICLE INFO

ABSTRACT

Migration of cells in the ocular surface underpins physiological wound healing as well as many human diseases. Transglutaminase (TG)-2 is a multifunctional cross-linking enzyme involved in the migration of skin fibroblasts and wound healing, however, its functional role in epithelial migration has not been evaluated. This study investigated the importance of TG-2 in a murine corneal wound healing model as well as the mechanistic role of TG-2 in the regulation of related biological processes such as cell adhesion and migration of cultured human corneal epithelial (HCE-T) cells. Corneal wound closure was delayed in homozygous TG-2 deleted mice compared to wild type mice. HCE-T cells that were knocked-down for TG-2 expression through stable expression of a short-hairpin (sh) RNA targeting TG-2, were delayed in closure of scratch wounds (48 compared to 12 h in control cells expressing scrambled shRNA). TG-2 knockdown did not influence epithelial cell cycle progression or proliferation, rather, it led to reduced epithelial cell adhesion, spreading and velocity of migration. At the molecular level, TG-2 knockdown reduced phosphorylation of β-3 integrin at Tyr747, paxillin at Ser178, vinculin at Tyr822 and focal adhesion kinase at Tyr925 simultaneous with reduced activation of Rac and CDC42. Phosphorylation of paxillin at Ser178A has been shown to be indispensable for the migration of corneal epithelial cells (Kimura et al., 2008) [18]. TG-2 dependent β-3 integrin activation, serine-phosphorylation of paxillin, and Rac and CDC42 activation may thus play a key functional role in enhancing corneal epithelial cell adhesion and migration during wound healing.

© 2013 Elsevier B.V. All rights reserved.

1. Introduction

Transglutaminase (TG)-2 [1] is a multi-functional cross-linking protein that is ubiquitously expressed [2,3]. It is able to covalently cross-link peptide substrates and also serve as a G protein [2]. Recently cell surface TG-2, localized at the basal and apical surfaces of cells and cell–cell contacts [4], has been implicated in cell–matrix interactions [5], which may affect cell adhesion and migration properties [6,7]. β-Integrins 1 and 3, vital for cell–matrix interactions, are colocalized with TG-2 and mediate outside-in signaling of cell surface TG-2 [8]. Although connective tissue structures (anchoring fibrils, microfibrils and collagen fibrils) that are linked to epithelial cells via hemidesmosomes

are crosslinking substrates of TG-2 [9], cell surface functions of TG-2 are not dependent on transamidase activity [4,10]. Thus, TG-2 can influence cell adhesion and migration through the other types of protein–protein interactions apart from catalyzing cross-linking of matrix substrates.

TG-2 is expressed in various ocular structures [11]. Previous work shows that TG-2 affects conjunctival inflammation and eosinophilic infiltration in a guinea pig model [12], it is involved in pterygium, a common ocular surface disease with fibrovascular proliferation and matrix anomalies [13], and it is up-regulated in the healing process in a rat corneal abrasion model [14].

The roles of TG-2 in various wound healing related processes are diverse [15] and include the regulation of matrix stability and scarring, platelet aggregation and angiogenesis during the various stages of wound healing. The role of TG-2 in wound healing in the ocular surface has not been evaluated. Wound healing in cornea will reduce transparency and affect visual function; hence it deserves to be evaluated as a

Abbreviations: Tg, Transglutaminase
* Corresponding author at: Singapore National Eye Center, 11 Third Hospital Avenue, Singapore 168751, Singapore. Tel.: +65 62277255; fax: +65 63224599.
E-mail address: Louis.tong.h.t@snec.com.sg (L. Tong).

unique scenario. Phosphorylation of paxillin, a key molecule in the cell-adhesion complex is vital for adhesion and migration of corneal epithelial cells [16]. Although TG-2 is known to signal through β-1 integrin to p190RhoGAP *via* phosphorylation of src kinase upon fibroblast adhesion [17], it is not known how TG-2 affects other proteins in the cell-adhesion complex.

In this study, we evaluated the role of TG-2 in a murine corneal wound healing model, as well as the mechanistic role of TG-2 in the regulation of related biological processes such as cell adhesion and migration of cultured human corneal epithelial cells.

2. Materials and methods

2.1. Mouse model of corneal wound healing

Mice were handled according to guidelines in the Association for Research in Vision and Ophthalmology Statement for the Use of Animals in Ophthalmic and Vision Research and protocols approved by the Institutional Animal Care and Use Committee of SingHealth. Heterozygous TG-2-deleted mice (Tgm2$^{tm1.1Rmgr}$) originally on a mixed C57BL/6J–129S1/SvImJ strain background were established as previously described [18] and backcrossed more than 12 generations to C57BL/6J to generate congenic heterozygote (TG-2$^{+/-}$) mice that share >99.95% genomic homogeneity with C57BL/6J. Congenic C57BL/6J TG-2$^{+/-}$ mice were bred to generate homozygous (TG-2$^{-/-}$) and wild type (TG-2$^{+/+}$) littermate founders. Mice were anesthetized by intraperitoneal injection of ketamine hydrochloride (2 mg/g body weight; Parnell Laboratories, Mascot, NSW, Australia) and xylazine (0.4 mg/g body weight; Troy Laboratories, Smithfield, NSW, Australia); depth of anesthesia was monitored by limb withdrawal using toe pinching. The central cornea was marked by a trephine 2 mm in diameter and the epithelium was peeled off using forceps under a dissecting microscope. Wound closure was assessed by fluorescein staining (5 s, sterile 1% Minims fluorescein sodium solution (Bausch & Lomb, Rochester, NY, USA; diluted 1:4 in sterile saline)) followed by sterile saline rinsing and digital camera photography in cobalt blue light with ultraviolet light filters. Wound area was determined (Kodak Molecular Imaging Software, Carestream Health Inc., Rochester, New York) and expressed as a percentage of total wounded corneal area.

2.2. Cell culture

Human SV-40 immortalized corneal epithelial cell line HCE-T (RCB 1384, Riken Cell Bank, Ibaraki, Japan) provided courtesy of Kaoru Araki-Sasaki (Kinki Central Hospital, Hyogo, Japan) [19] was used at passages 88 to 98. All cell lines were cultured in DMEM-F12/5% FBS (Invitrogen, Grand Island, NY, USA) in a humidified 5% CO$_2$ incubator at 37 °C with fresh medium replaced every 2 days.

2.3. Stably transfected cell lines

HCE-T cells stably transduced with shRNA targeting TG-2 (referred to as shRNA TG-2) and HCE-T cells stably transduced with non-specific scrambled shRNA (referred to as scrambled shRNA) were described previously [20].

2.4. Measurement of cell area

shRNA TG-2 or scrambled shRNA stably-transfected HCE-T cells were cultured on uncoated or fibronectin-coated dishes with serum-supplemented medium until 80% confluency, incubated in serum-free medium overnight, then seeded into uncoated or fibronectin pre-coated 8-well chamber slides (BD Biosciences, MA, USA) overnight. Using ImageJ software (National Institute of Health, USA), cell boundaries including cytoplasmic protrusions of non-overlapping cells were

outlined manually on captured images (20× magnification, Axioplan 2 fluorescence microscope, Carl Zeiss, Oberkochen, Germany) and cell area was measured. Nuclear boundaries of the same cells were drawn to calculate nuclei areas.

2.5. Scratch wound assay

shRNA TG-2 or scrambled shRNA stably-transfected HCE-T cells were seeded in duplicate in uncoated or fibronectin-coated 6-well tissue culture plates and grown for 24 h to produce a confluent monolayer of cells. Nine straight scratches were made with a 1 mL blue pipette tip. Re-epithelialization of the denuded area was determined (ImageJ software) from images captured at fixed positions every 2 h for 14 h.

2.6. Two-D cell migration assay

shRNA TG-2 or scrambled shRNA stably-transfected HCE-T cells were seeded in a 6 mm culture glass cylinder (Bioptechs, PA, USA) filled with serum-supplemented medium. After overnight incubation, the culture cylinder was removed and cell migration was recorded every 10 min for 100 frames (around 16 h). Cell centroids were computed after manually outlining cells using ImageJ software.

2.7. Cell trypsinization assays

Cells were washed with phosphate buffered saline (PBS, 1st base, Singapore), incubated with PBS-diluted 0.005% Trypsin-EDTA (Sigma, Saint Louis, MO, USA) at 37 °C, 5% CO$_2$ for 1 h and photographed periodically without mechanical perturbation.

2.8. Cell impedance studies

Cell impedance properties were monitored using the Xcelligence system (Roche Applied Science, Basel, Switzerland), which dynamically monitors cell events in real-time. The presence of cells on top of electrodes affects the local ionic environment at the electrode/solution interface, leading to an increase in electrode impedance, which is displayed as cell index (CI) values [21].

2.9. Cell proliferation assays

Cell proliferation/viability was assessed by 3-(4,5-imethylthiazol-2-yl)-5-(3-carboxymethoxyphenyl)-2-(4-sulfophenyl)-2H-tetrazolium (MTS) colorimetric assay using the CellTiter 96® Aqueous One Solution Cell Proliferation assay (Promega, Madison, WI, USA). Cell proliferation was also analyzed 3 to 8 h after the scratch test by Ki-67 staining of cells fixed as for immunofluorescent staining below. Positively-stained cells (green) within contiguous cells of a confluent area were counted 3 times in each cell type.

2.10. Immunofluorescence staining

This was performed as previously described [22]. Briefly, cultured cells were fixed (4% paraformaldehyde, room temperature, 15 min), blocked for non-specific binding (30 min), appropriate primary antibody, then secondary antibody was added. Table 1 lists primary and secondary antibodies used.

For mouse tissue, 10 μm cryostat sections were placed on poly-L-lysine-coated slides, fixed (4% paraformaldehyde, 20 min), rinsed (PBS), permeabilized (30 min, 0.15% Triton X-100; Sigma), blocked (30 min, 4% bovine serum albumin BSA; Sigma), incubated with primary antibody (mouse phospho Ser178 paxillin, 30 min, room temperature in moist chamber), rinsed (PBS) and incubated with FITC conjugated secondary antibody (20 min, room temperature in moist chamber). After rinsing (PBS), samples were embedded in

Table 1
List of antibodies used.

Antigen	Antibody (catalog number)	Dilution	Species	Source
Transglutaminase 2	ab421	1: 50 (IF[a])	Rabbit	Abcam
Anti-(Ki) 67	18-0191Z	1:40 (IF[a])	Rabbit	Invitrogen
Phospho-β3 integrin (Tyr747)[b]	ab38460	1: 400 (western)	Rabbit	Abcam
		1: 50 (IF[a])		
Phospho-β1 integrin (S785)	ab5185	1: 200 (western)	Rabbit	Abcam
Phospho-vinculin integrin (Tyr 822)	V4889	1: 1000 (western)	Rabbit	Sigma
		1: 50 (IF[a])		
Phospho-Paxillin (S178)	A300-100A	1: 1000 (western)	Rabbit	Bethyl Laboratories
		1: 100 (IF[a])		
Phospho-FAK (Tyr576)	#07-157	1: 150 (western)	Rabbit	Millipore
Phospho-FAK (Tyr925)	#3284	1: 500 (western)	Rabbit	Cell Signaling
Integrin β3	ab34409	1: 400 (western)	Mouse	Abcam
Integrin β1	MAB1965	1: 200 (western)	Mouse	Millipore
Vinculin clone hVIN-1	V4505	1: 400 (western)	Mouse	Sigma
Paxillin	P1093	1: 500 (western)	Mouse	Sigma
FAK	610087	1: 200 (western)	Mouse	BD Biosciences
Talin	T3287	1: 500	Mouse	Sigma
β-Actin	ab8227	1: 1000	Rabbit	Abcam
Anti-mouse IgG (whole molecule) FITC	F2012	1: 800	Goat	Sigma
Anti-rabbit Alexa Fluor 488	A11070	1: 800	Goat	Invitrogen
Anti-mouse HRP	A9044	1: 5000	Goat	Sigma
Anti-rabbit HRP	A0545	1: 5000	Goat	Sigma

[a] Immunofluorescence staining.
[b] Although called integrin beta 3-phospho-Y773 antibody in manufacturer's catalog, it refers to the same tyrosine residue because amino acid counting starts from N terminus of propeptide.

UltraCruzTM mounting medium with DAPI (Santa Cruz, California, USA). Tissue sections not incubated with primary antibody were used as negative controls.

2.11. Western blot

This was performed as previously described [20]. Scrambled shRNA (8×10^5) and shRNA TG-2 (1×10^6) stably-transfected HCE-T cells cultured in serum-supplemented medium until 60–70% confluency were passaged and seeded to 60–70% confluency overnight in serum-free medium in a new culture vessel. After aspiration of culture medium, cells were washed three times in PBS, placed on ice and freshly prepared RIPA lysis buffer (50 mM Tris–HCL, pH 7.4, 1% NP40, 0.5% sodium deoxycholate, 0.1% SDS, 150 mM sodium chloride, 2 mM EDTA, and 50 mM sodium fluoride) containing a cocktail of protease and phosphatase inhibitors (Sigma-Aldrich and Roche) was added. Cells were gently scraped and collected. Protein concentration was measured using the micro-BCA method. Sample buffer containing β-mercaptoethanol was added to 70 μg of protein for each sample and heated to 95 °C for 5 min. Subsequent SDS-PAGE and transfer to immunoblots were performed as previously described [20]. Table 1 lists primary and secondary antibodies used.

2.12. Cell cycle analysis

4×10^5 cells were cultured for 2 days. Non-adherent and trypsinized cells were pelleted, resuspended in 500 μL PBS, transferred drop by drop to 4.5 mL of chilled ethanol while gently vortexing, incubated in ethanol (overnight, 4 °C), pelleted, resuspended in PBS (5 mL, room temperature, 1 min), pelleted by centrifugation and resuspended in GUAVA cell cycle reagent (Millipore, MA, USA) at a concentration recommended by the manufacturer, followed by 30 min room temperature incubation before analysis by mini-flow cytometry (GUAVA, Millipore). Data were analyzed by ExpressPro software.

2.13. Rho (RhoA, Cdc42 and Rac) protein activation assays

Small G-protein activity (G-LISA Assays, Cytoskeleton, Denver, USA) was measured in stably-transfected HCE-T cells expressing

shRNA TG-2 or scrambled shRNA that were cultured until 50% confluency in 5% FBS medium. Serum in the medium was used as recommended by the manufacturer (Cytoskeleton) as one of the known Rho activators to stimulate Rho protein activity in the cultured cells.

2.14. Statistical analysis

For continuous variables, all results shown are means ± SD. Statistical differences for cell areas were determined by ANOVA with post-hoc comparisons where the ANOVA is significant. The general linear model (GLM) procedure was used (SPSS, Inc.) for the evaluation of velocity of cell migration and gap width in *in vitro* scratch assays. The post hoc test option in the GLM procedure was used to evaluate for significant differences between the 4 conditions (cells with scrambled shRNA and shRNA targeting TG2, either with or without fibronectin), p values adjusted for multiple comparisons were evaluated for statistical significance. For categorical variables, proportions (*e.g.* proportions of positively-labeled Ki-67 cells) were compared using the Chi square test, with $p \leq 0.05$ being considered significant.

3. Results

A uniform area of the corneal surface was abraded in wild type ($TG-2^{+/+}$) and homozygous TG-2 deleted ($TG-2^{-/-}$) mice. Although the time taken to repair the corneal epithelium varied depending on wound depth and the way mechanical abrasion was performed, fluorescein staining of the cornea denuded of epithelium indicated corneal wound closure was consistently delayed in $TG-2^{-/-}$ mice compared to $TG-2^{+/+}$ (Fig. 1A). Epithelial healing was completed after 7 days in $TG-2^{-/-}$ compared to 4 days in $TG-2^{+/+}$ (Fig. 1B) with statistically significant differences ($p < 0.05$) in residual epithelial wound area from day 3 onwards. Immunofluorescence staining detected TG-2 in corneal epithelial layers and basement membrane of $TG-2^{+/+}$ mice but not in $TG-2^{-/-}$ mice (Fig. 1C). During the healing process, it was observed that the new corneal epithelial cell sheet in $TG-2^{-/-}$ mice was very friable and less adherent to the corneal bed than in $TG-2^{+/+}$ mice.
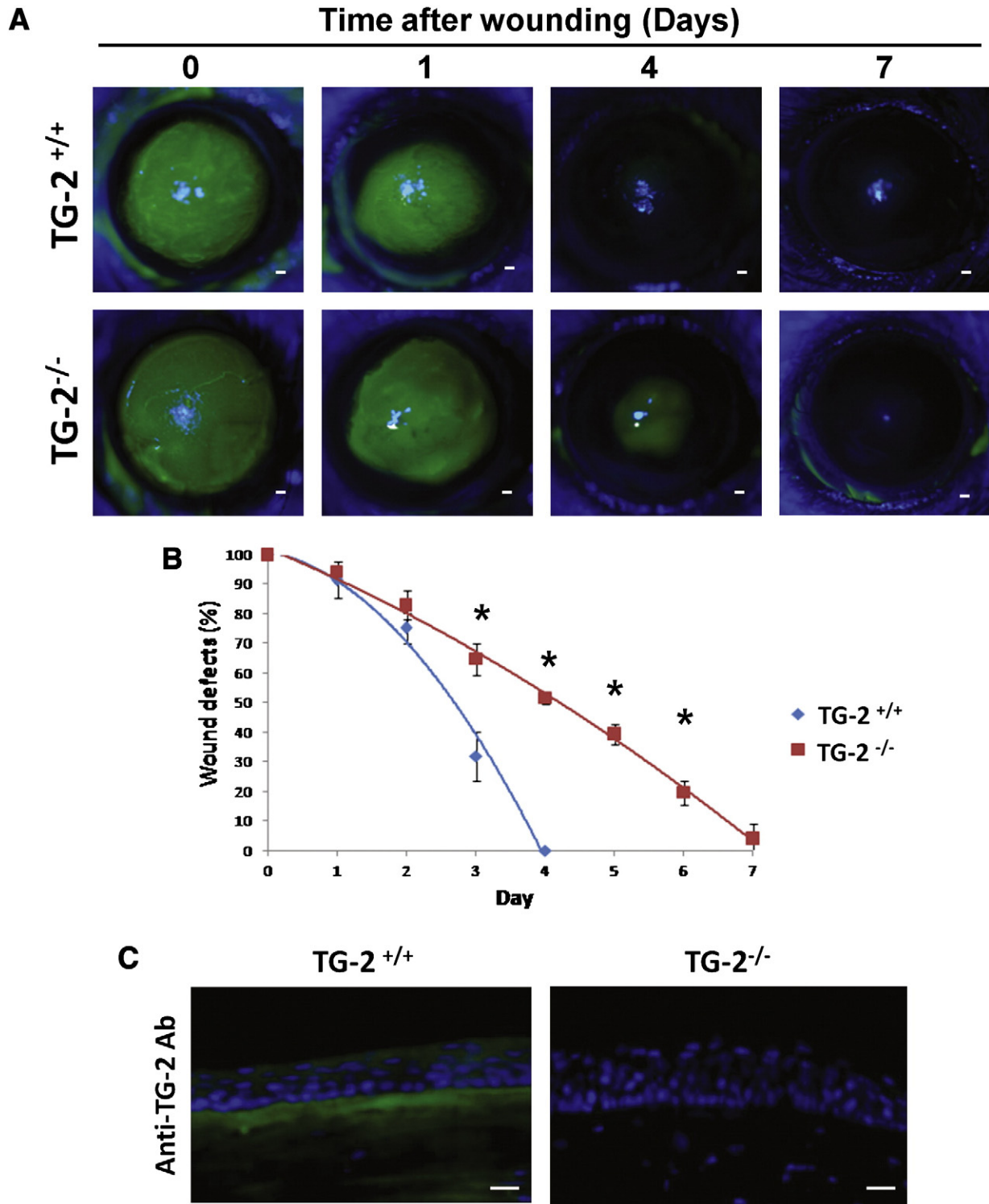
Fig. 1. Deletion of TG-2 from corneal epithelial layers and the basement membrane results in delayed corneal wound closure in homozygous transglutaminase (TG)-2 deleted (TG-2$^{-/-}$) mice relative to wild type control (TG-2$^{+/+}$) mice. (A) Representative microscopy images of murine cornea following the removal of corneal epithelium from TG-2$^{+/+}$ and TG-2$^{-/-}$ mice and topical fluorescein staining of the epithelial defect (green). Scale bar = 100 μm. (B) Percentage of wound defect remaining (vertical axis) over time (horizontal axis) in TG-2$^{+/+}$ and TG-2$^{-/-}$ mice, n = 5 for each genotype from 3 independent experiments. *: p < 0.05. (C) Representative immunofluorescence staining of central unwounded TG-2$^{+/+}$ and TG-2$^{-/-}$ mouse corneas with primary antibody against TG-2 and FITC conjugated secondary antibody (green) and with DAPI nuclear counterstaining (blue). Scale bar = 50 μm.

Due to the prohibitively high cost of primary murine corneal epithelial cell culture medium the high volume of cells required for various assays, batch to batch variability of phenotype of primary cells upon passaging, as well as the translational medicine implications of using human cells, we investigated this further *in vitro* using immortalized human corneal epithelial (HCE-T) cells stably transfected with shRNA against TG-2 or with scrambled shRNA. The specificity of the shRNA against TG-2 was confirmed by us previously by showing that TG-2

transcript and protein are greatly reduced in HCE-T cells by this shRNA [20], as is cell surface TG-2 expression (Supplementary File 1), and that the functional effect of this reduction can be overcome by selectively over-expressing wild type TG-2 [20]. In a scratch test assay, although cell density was similar (p > 0.05, data not shown), shRNA TG-2-expressing cells displayed delayed closure of a uniform width scratch wound, with closure not evident until 48 h compared to 12 h in scrambled shRNA-expressing cells (Fig. 2A). This phenomenon was independent of fibronectin pre-coating of the culture vessel (Fig. 2A). The difference in width of the residual wound between the two stably transfected cell lines was statistically significant (p < 0.05) from 6 h after scratching (Fig. 2B). Upon general linear model (GLM) analysis

(2–14 h after scratching) the 'within subject' effect (time) was significant (p < 0.001) and the TG-2 status and fibronectin coating were significant 'between subject' effects (p < 0.001). On post-hoc testing, control cells grown on fibronectin closed the wound significantly faster than shRNA TG-2-expressing cells on fibronectin (p = 0.001) or shRNA TG-2-expressing cells on uncoated plates (p = 0.005). Control cells cultured on uncoated plates closed the wound faster than shRNA TG-2-expressing cells on uncoated plates (p = 0.004) or shRNA TG-2-expressing cells on fibronectin-coated plates (p = 0.001). There was no significant difference in wound width between shRNA TG-2-expressing cells cultured on plates with or without fibronectin (p = 0.885).
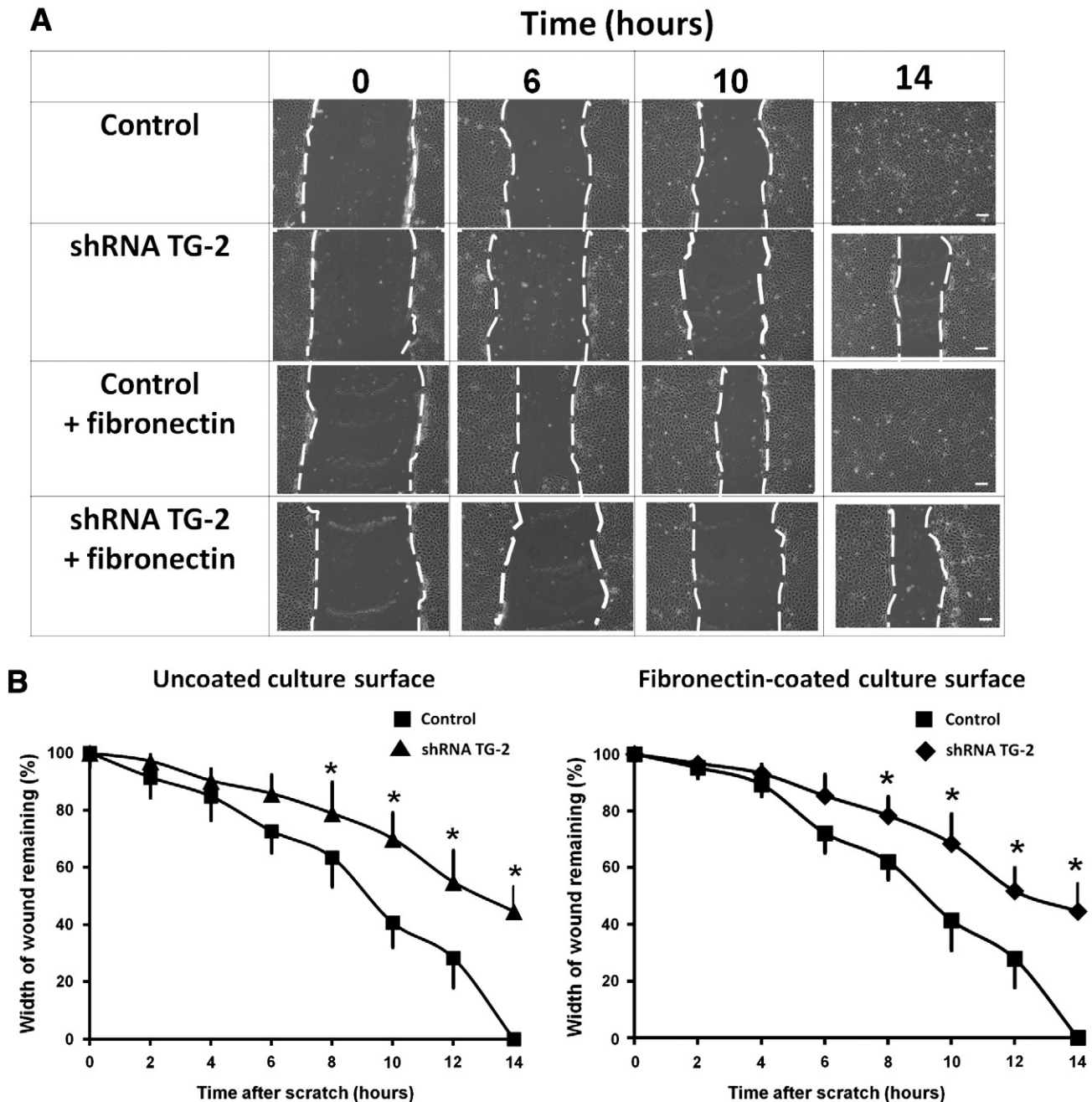
Fig. 2. Knockdown of TG-2 in corneal epithelial cells results in delayed closure of a scratch wound. (A) Representative phase contrast microscopy images taken at various time intervals after a single uniform width scratch wound of confluent HCE-T cells stably transfected with a scrambled shRNA (control) or a TG-2-targeting shRNA (shRNA TG-2), seeded on either uncoated or fibronectin-coated surfaces. Scale bar = 50 μm. (B) Graph showing the percentage width of wound remaining (vertical axis) over time (horizontal axis), n = 6 independent experiments. *: p < 0.05.

A
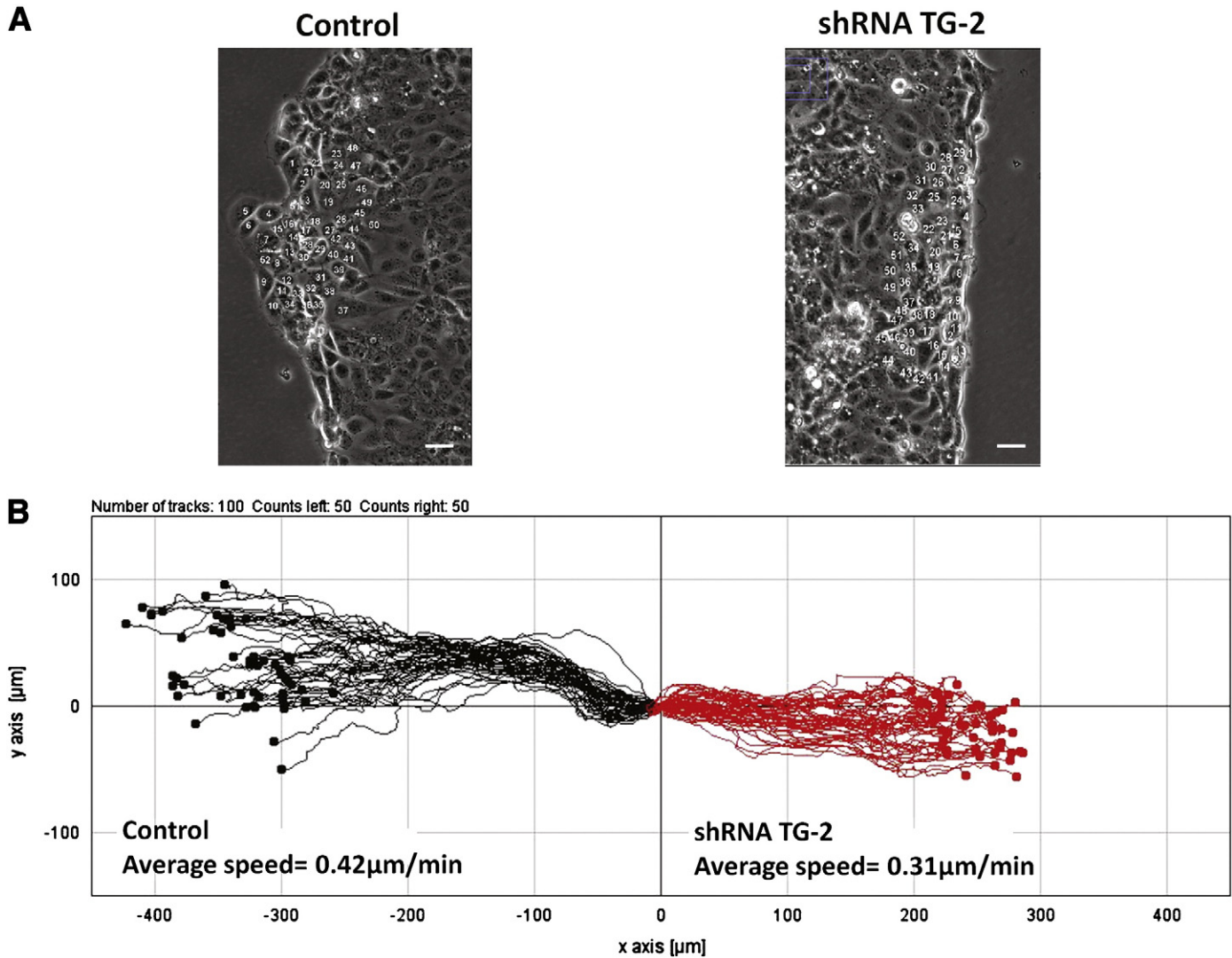
Fig. 3. Knockdown of TG-2 in corneal epithelial cells results in decreased velocity of cell migration. (A) Representative phase contrast microscopy images taken immediately after the commencement of cell migration in HCE-T cells stably transfected with scrambled shRNA (control) or shRNA targeting TG-2 (shRNA TG-2), seeded on uncoated plates. This is a non-traumatic cell migration assay (see 'Materials and methods'). Scale bar = 50 μm. (B) Cell migration depicted as line plot of centroid positions of 50 randomly selected contiguous cells at the advancing edge, tracked every 10 min over 16 h by live cell time-lapse microscopy. Initial cell positions were normalized to plot origin. A representative experiment from 3 independent experiments is shown.

A 2-D cell migration assay was used to investigate if this delay in wound closure reflected a lower migration speed of shRNA TG-2-expressing cells. On uncoated plates, scrambled shRNA-expressing cells had significantly higher velocity of movement (average speed of 0.42 ± 0.051 μm/min) compared to shRNA TG-2-expressing cells $(0.31 \pm 0.033$ μm/min; $p < 0.0001$; Fig. 3 and Supplementary File 2), the difference in migration speed between scrambled shRNA- and shRNA TG2-expressing cells being 0.42–0.31 or 0.11 μm/min. On fibronectin-coated plates, the difference in migration speed between scrambled shRNA- and shRNA TG2-expressing cells was 0.66–0.54 or 0.12 μm/min (data not shown, lower magnification images shown in Supplementary File 3). Upon GLM analysis with cell velocity at each time interval (10 min segments repeated 99 times) as the dependent variable, the 'between subject' factors (fibronectin status and TG-2 status) were significant ($p = 0.001$). The time effect is significant ($p < 0.001$) and probably reflects increased velocity in the first 25 time points (first 4 h) (Supplementary File 4). On post hoc testing, control cells migrated faster on fibronectin than the other 3 conditions (all $p < 0.001$); control cells on uncoated plates migrated significantly faster than shRNA TG-2-expressing cells on uncoated plates ($p < 0.001$),

and shRNA TG-2-expressing cells on fibronectin migrated faster than on uncoated plates ($p < 0.001$). There was no difference in velocity between control cells on uncoated plates and shRNA TG-2-expressing cells on fibronectin-coated plates ($p = 1.0$). There was also a tendency for cells that expressed shRNA against TG-2 to be less adherent to the underlying culture vessel, appearing as a loose sheet folding back on itself at the margin of advancing cells.
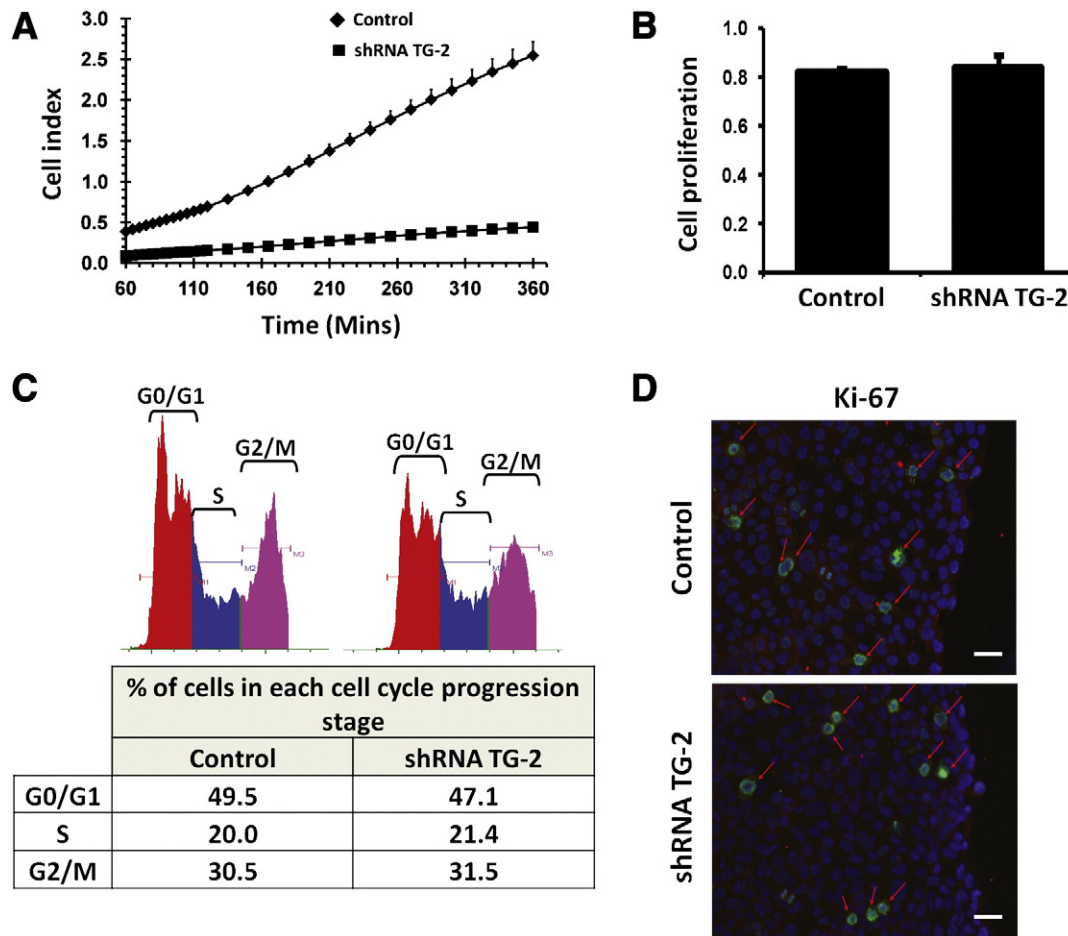
One to six hours after seeding on uncoated plates, cells expressing shRNA against TG-2 were significantly reduced in cell impedance, which measures cell properties such as cell number or adhesion/area (Fig. 4A), relative to cells expressing scrambled shRNA (TG-2 status $p < 0.001$). Each of the parameters potentially contributing to the reduced cell impedance of shRNA TG-2-expressing cells was then analyzed separately. Firstly, MTS assay of cell proliferation in preconfluent monolayers seeded on uncoated plates (Fig. 4B) and steady state cell cycle progression (Fig. 4C) indicated no difference in proliferation rates. Consistent with these findings, 6 h after a scratch wound the proportion of proliferating (Ki-67 positive) cells was low (presumably still due to the effects of contact inhibition prior to scratching) and was not significantly different ($p = 0.59$) between

cells expressing scrambled shRNA [11/368 (95%CI: 0.0156–0.0550)] and cells expressing shRNA against TG-2 [14/581 (95%CI: 0.0136–0.0415)] (Fig. 4D). When individual single cells near the scratch wound were tracked over 24 h, 1–2/50 cells divided. Secondly, using time-lapse photography, the rate of cell detachment from uncoated plates after trypsinization (Fig. 4E and Supplementary File 5) was greater in cells expressing shRNA against TG-2 than in cells expressing scrambled shRNA. We acknowledge that this result may not be robust in the absence of a directional shearing force. Lastly, the mean area of individual phalloidin-stained cells measured 24 h after attachment on fibronectin-coated plates was 555 ± 161 μm² for cells expressing shRNA against TG-2 compared to 682 ± 218 μm² for cells expressing scrambled shRNA ($p < 0.001$). Interestingly, there was no difference in cell area on uncoated plates (Fig. 4F), nor was there a difference in nuclei area between groups ($p > 0.05$ ANOVA in Fig. 4F). Together, these findings indicate that the delayed scratch wound closure rate of cells expressing shRNA TG-2, relative to scrambled RNA, may be attributable to differential cell adhesion, spreading and/or migration, but not proliferation.

Adhesion and directional migration of epithelial cells during wound healing involve integrin activation, which mediates actin stress fiber aggregation and formation of adhesion complexes in the leading edge. To investigate the actin cytoskeleton of epithelial cells expressing scrambled shRNA or shRNA against TG-2, filamentous (F)-actin was fluorescently stained using phalloidin, 3 h (Fig. 5) and 6 h (data not shown) after the scratch wound. At both time points, cells expressing scrambled shRNA showed strong condensation of F-actin around the cortex of advancing cells as well as over cell–cell junctions, with most cells forming lamellipodia in the direction of cell movement. In cells expressing shRNA against TG-2, however, the pattern of F-actin was more disrupted at both time points, with the detachment of individual cells at the advancing edge, and extension of lamellipodia not just towards the direction of the wound but also at right angles to this (arrow in Fig. 5). This suggests that some cells may have detached due to defective adhesion between the cell and underlying substrate.

Next we investigated the role of TG-2 in phosphorylation of integrins and various components of focal adhesion complexes in epithelial cells expressing scrambled shRNA or shRNA against TG-2, plated in serum-free medium overnight to 60–70% confluency on uncoated plates (Fig. 6A–F). These experiments were repeated with cells seeded on fibronectin-coated plates for 5 h and similar results

% of cells in each cell cycle progression stage		
	Control	shRNA TG-2
G0/G1	49.5	47.1
S	20.0	21.4
G2/M	30.5	31.5

Fig. 4. Knockdown of TG-2 in corneal epithelial cells results in decreased cell impedance due to decreased strength of adhesion and decreased cell spreading, with no effect on proliferation. (A) HCE-T cells stably transfected with scrambled shRNA (control) or shRNA targeting TG-2 (shRNA TG-2) were seeded (5×10^3 cells/200 mL DMEM-F12/5% FBS) in triplicate on uncoated plates and monitored non-invasively for cell impedance (cell index) over time. (B) MTS cell proliferation assay of control and shRNA TG-2 cells seeded on uncoated plates. Cell proliferation (y-axis) was measured at A490. (C) Cell cycle analysis of control or shRNA TG-2 cells using propidium iodide to measure the percentage of cells in G0/G1, S, and G2/M phases by mini-flow cytometry. (D) Representative microscopy images of Ki-67 staining (green) to monitor cell proliferation (red arrows) 6 h after a single uniform width scratch wound of confluent control or shRNA TG-2 cells, seeded on uncoated plates. Blue, DAPI-stained cell nuclei. Scale bar = 50 μm. (E) Representative time-lapse microscopy images of control and shRNA TG-2 cells on uncoated dishes after the addition of diluted trypsin. Imaging was discontinued after 25 min for shRNA TG-2 or after 50 min for control, when all cells had detached. Detached cells are rounded and clumped together. (F) Cell (top) and nuclei (bottom) area of control or shRNA TG-2 cells seeded for 24 h on fibronectin-coated (+) or uncoated (−) plates. More than 500 attached cells were selected over 3 independent experiments.*: $p < 0.001$.
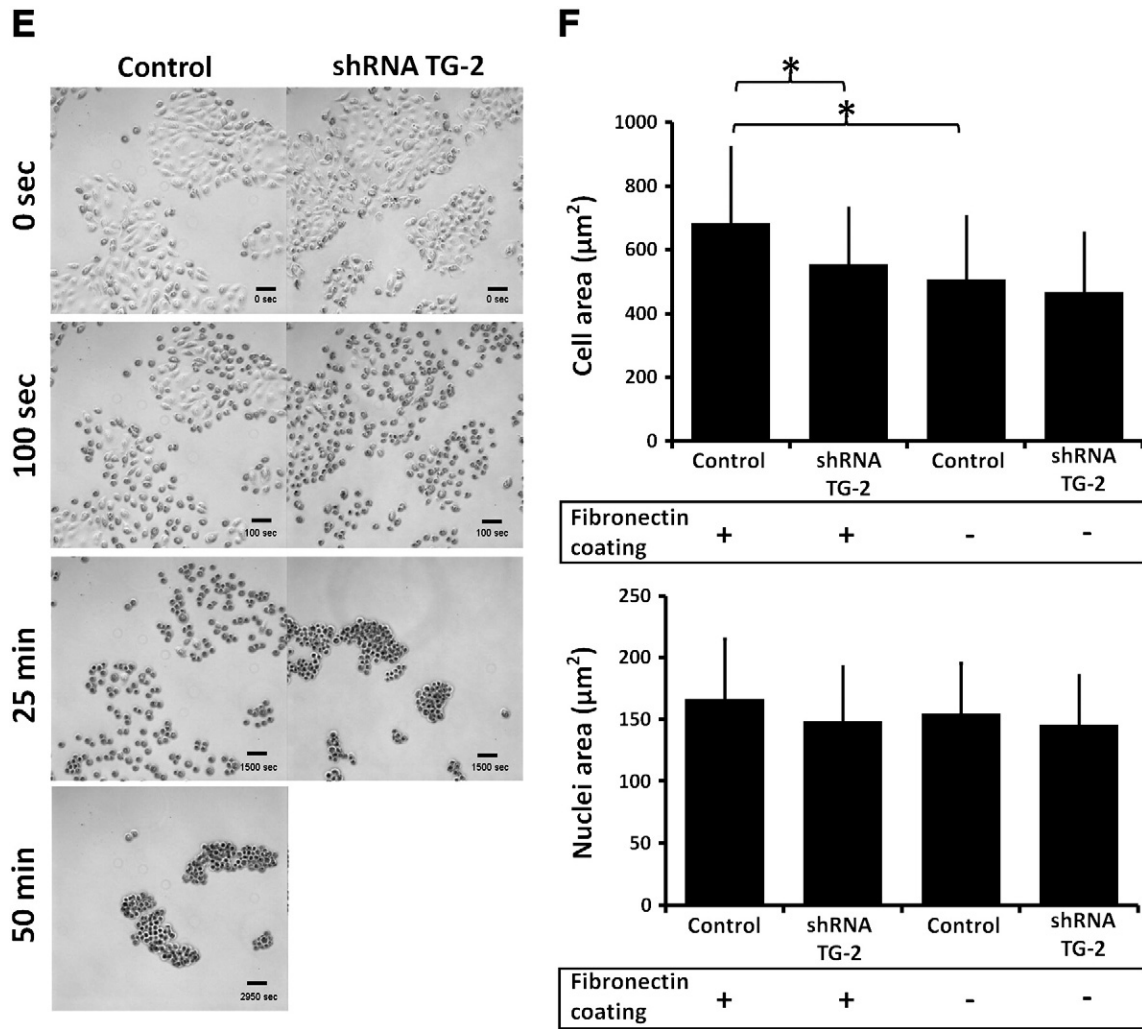
Fig. 4 (*continued*).

were obtained (Supplementary File 6). Fig. 6A shows that phosphorylation of β-1 integrin (a known component of the early cell–matrix adhesion complex) at Ser785 was not affected by the TG-2 status of the cells. Similar results were obtained for cells grown on fibronectin-coated plates (data not shown). Although β-3 integrin (another component of the adhesion complex) has been reported to be absent from corneal epithelial cells [23], we were able to detect β-3 integrin by Western blot in these cells (Fig. 6B) as well as in cultured primary corneal epithelial cells grown from cadaveric limbal explant tissue (Supplementary File 7A). In a separate GeneChip study, we also found β-3 integrin transcripts in our corneal epithelial cell line as well as in primary cultured corneal epithelial cells (Supplementary File 7B). Moreover, phosphorylation of β-3 integrin at Tyr747 was reduced in cells expressing shRNA against TG-2 compared to cells expressing scrambled shRNA (Fig. 6B). Reduced phosphorylation was also observed for paxillin (another early adhesion complex component) at Ser178 (Fig. 6C), vinculin (a component of the late adhesion complex) at Tyr822 (Fig. 6D) and focal adhesion kinase (FAK) at Tyr925, but not at Tyr576 (Fig. 6E) in cells expressing shRNA against TG-2, relative to control cells expressing scrambled shRNA. Because we observed less cell spreading (Fig. 4F) on fibronectin-coated, but not uncoated, plates in cells expressing shRNA TG-2 relative to control shRNA, we compared the phosphorylation level of one of these components (paxillin phosphorylation at

Ser178) in cells plated in serum-free medium overnight on uncoated *versus* fibronectin-coated plates, and found similar levels of decreased paxillin phosphorylation in cells expressing shRNA TG-2 relative to control shRNA (data not shown). Consistent with these results, following the abrasion of the corneal surface of TG-2$^{+/+}$ and TG-2$^{-/-}$ mice, less phosphorylated paxillin was observed at the advancing edge of corneal epithelium after 4 h and in repaired epithelium after 120 h in TG-2$^{-/-}$ mice relative to TG-2$^{+/+}$ mice (Fig. 6G).

Since nascent adhesion formation near the leading edge of lamellipodia involves the activation of small GTPases, Rac and CDC42, we investigated the level of activation of these proteins in subconfluent cultures. Activation of RhoA was not affected by TG-2 status, whereas activation of Rac and CDC42 was reduced in cells expressing shRNA against TG-2 compared to cells expressing scrambled shRNA (Fig. 6H).

4. Discussion

Using both an *in vivo* mouse model of corneal abrasion (Fig. 1) and a scratch wound of human corneal epithelial cells *in vitro* (Fig. 2) we show for the first time that corneal epithelial wound healing is enhanced by TG-2. TG-2 does not influence epithelial cell cycle progression or proliferation (Fig. 4B–D), rather, TG-2 enhances epithelial cell adhesion, spreading (Fig. 4E–F) and velocity of migration

Control   shRNA TG-2
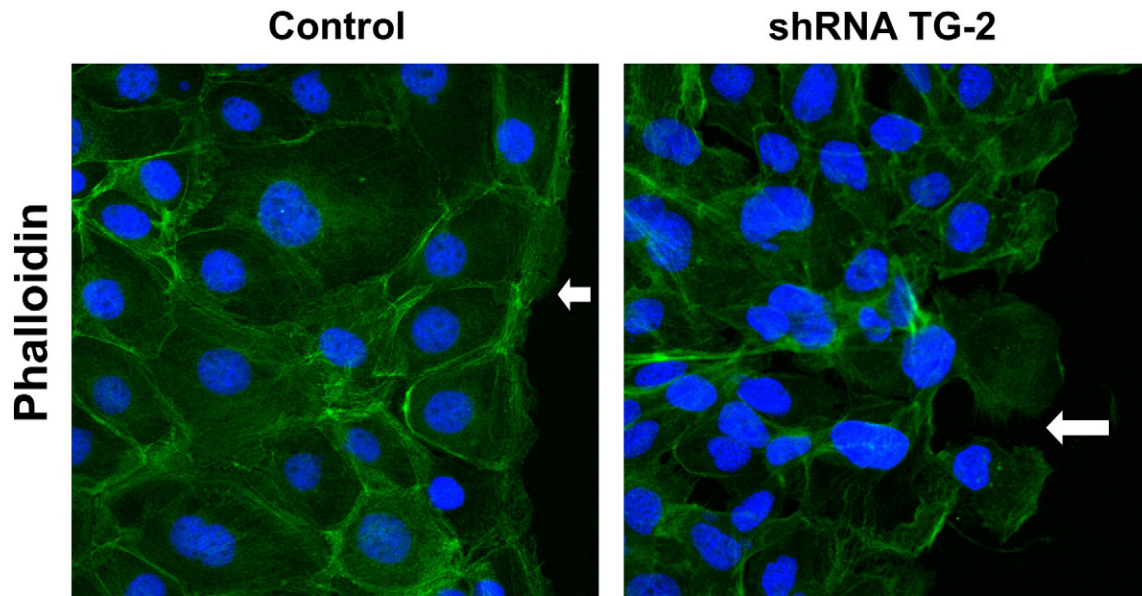
Fig. 5. Knockdown of TG-2 in corneal epithelial cells results in actin cytoskeleton changes. Representative fluorescence staining, using FITC-conjugated phalloidin (green), of an *in-vitro* scratch wound 3 h post wounding of cultured HCE-T cells stably transfected with scrambled shRNA (control) or shRNA targeting TG-2 (shRNA TG-2) seeded on uncoated plates. Nuclei were counterstained with DAPI (blue). White arrows indicate the direction of lamellipodia at the leading edge. Scale bar = 50 μm.

(Fig. 3B). Given that cell adhesion and spreading, especially in the leading edge of cytoplasmic processes, are critical to cell movement [24], the observed effect on epithelial cell migration of TG-2 reduction or absence likely reflects defective adhesion. This role of TG-2 is consistent with previous work describing cell surface TG-2 involvement in migration and/or adhesion of monocyte [8], retinal pigment epithelial cell [25], endothelial [26], osteoblast [27], breast cancer [28] and metastatic melanoma [29] cells. Interestingly, cell spreading area of corneal epithelial cells expressing shRNA against TG-2 was significantly reduced when plated on Fn-coated plates, but was comparable to control cells expressing scrambled shRNA when plated on uncoated plates. A similar observation has been noted in human endothelial cells stably transfected with antisense TG-2 cDNA [26]. Enhanced cell spreading on fibronectin-coated relative to uncoated plates is likely mediated through the direct interaction of TG-2 with fibronectin [30] in complex with integrins [5].

Although it is accepted that corneal epithelium contains β-1 but lacks β-3 integrin [23], we provide evidence using a well-characterized antibody against β-3 integrin and phosphoTyr747 of β-3 integrin, that β-3 integrin is indeed present in, and is activated in a TG-2-dependent manner upon the adhesion of, the cultured corneal epithelial cell line, HCE-T (Fig. 6). In addition, we found expression of β-3 integrin transcript and protein in primary human corneal epithelial cells cultured from cadaveric limbal explants, as well as in the corneal epithelial cell line HCE-T (Supplementary File 7).

Phosphorylation of the tail of β-3 integrin at Tyr747 plays important roles in both inside-out and outside-in signaling [31] and recruitment of signaling components [32] during cell adhesion on tissue culture plastic or matrix components [33]. Consistent with this matrix-independent activation of β-3 integrin, cells expressing shRNA against TG-2 were observed to have reduced phosphorylation of focal adhesion complex protein paxillin at Ser178, relative to cells expressing scrambled shRNA, on uncoated or fibronectin-coated plates (Fig. 6C, data not shown). Given mutation of Ser178 of paxillin to Ala inhibits the migration of the same line of human corneal epithelial cells as we used in our study [16] and, moreover, that less Ser178-phosphorylated paxillin was also observed at the delayed advancing edge of corneal epithelium in TG-2$^{-/-}$ than in TG-2$^{+/+}$ mice following the abrasion of the corneal surface (Fig. 6G), our study strongly suggests that the mechanism by which TG-2 mediates corneal epithelial wound closure involves serine phosphorylation of paxillin (Fig. 7). Phosphorylation of vinculin at Tyr822 and of FAK at Tyr925, but not Tyr576, was also TG-2-dependent (Fig. 6D, E). Of the three tyrosine residues in FAK that have been studied in the context of strain-induced epithelial cell migration, only phosphorylation of Tyr925 is required for downstream signaling through the PI3K/Akt axis independent of Src activation but dependent on Rac1 activation [34]. Rac and CDC42 are active in actin polymerization in the leading edge of moving cells [35], and their inhibition leads to the disruption of lamellipodia and filopodia formation [36,37]. Consistent with TG-2-dependent

Fig. 6. Deletion or knockdown of TG-2 in corneal epithelial cells results in reduced phosphorylation of a number of components of focal adhesion complexes as well as reduced activation of GTPases, Rac and CDC42. (A–F) Representative Western blots of total cell lysates (50 μg) from HCE-T cells stably transfected with scrambled shRNA (control) or shRNA targeting TG-2 (shRNA TG-2) that were seeded in serum-starved conditions to 70% confluency on uncoated plates, probed with primary antibodies against (top panels) (A) β-1 integrin phosphorylated at Ser785 (pS785 β-1 integrin) and total β-1 integrin, (B) β-3 integrin phosphorylated at Tyr747 (pTyr747 β-3 integrin) and total β-3 integrin, (C) paxillin phosphorylated at Ser178 (pS178 paxillin) and total paxillin, (D) vinculin phosphorylated at Tyr822 (pTyr822 vinculin) and total vinculin (E) focal adhesion kinase (FAK) phosphorylated at Tyr925 (pTyr925 FAK) or Tyr576 (pTyr576 FAK) and total FAK, and (bottom panel) β-actin as loading control. (F) Bar chart showing the normalization of densitometry of Western blots from 3 to 5 independent experiments. Anti-phospho-specific epitope intensities were normalized to anti-total intensities of the respective adhesion proteins (total integrin, paxillin, vinculin, FAK) and expressed as fold change in the intensity of control cells. *p < 0.05 using the Mann Whitney *U* test (G) Representative immunofluorescence images of fresh frozen mouse cornea from TG-2$^{+/+}$ and TG-2$^{-/-}$ mice 4 h (top row) and 120 h (bottom row) post-wounding, stained with primary antibodies against paxillin phosphorylated at Ser178, followed by FITC-conjugated secondary antibody (green). Nuclei were counterstained with DAPI (blue). Red arrows indicate the advancing edge of corneal epithelium, white arrows indicate the margin of prominent staining of phosphorylated paxillin. Scale bar = 50 μm. (H) Activity assays for Rac (left), CDC42 (middle) and RhoA (right). Lysates from shRNA TG-2 and control cells, cultured to 50% confluency on uncoated plates, were assayed in G-LISA assays according to manufacturer's instructions and absorbance read at 490 nm (n = 3 independent experiments). *: p < 0.05.
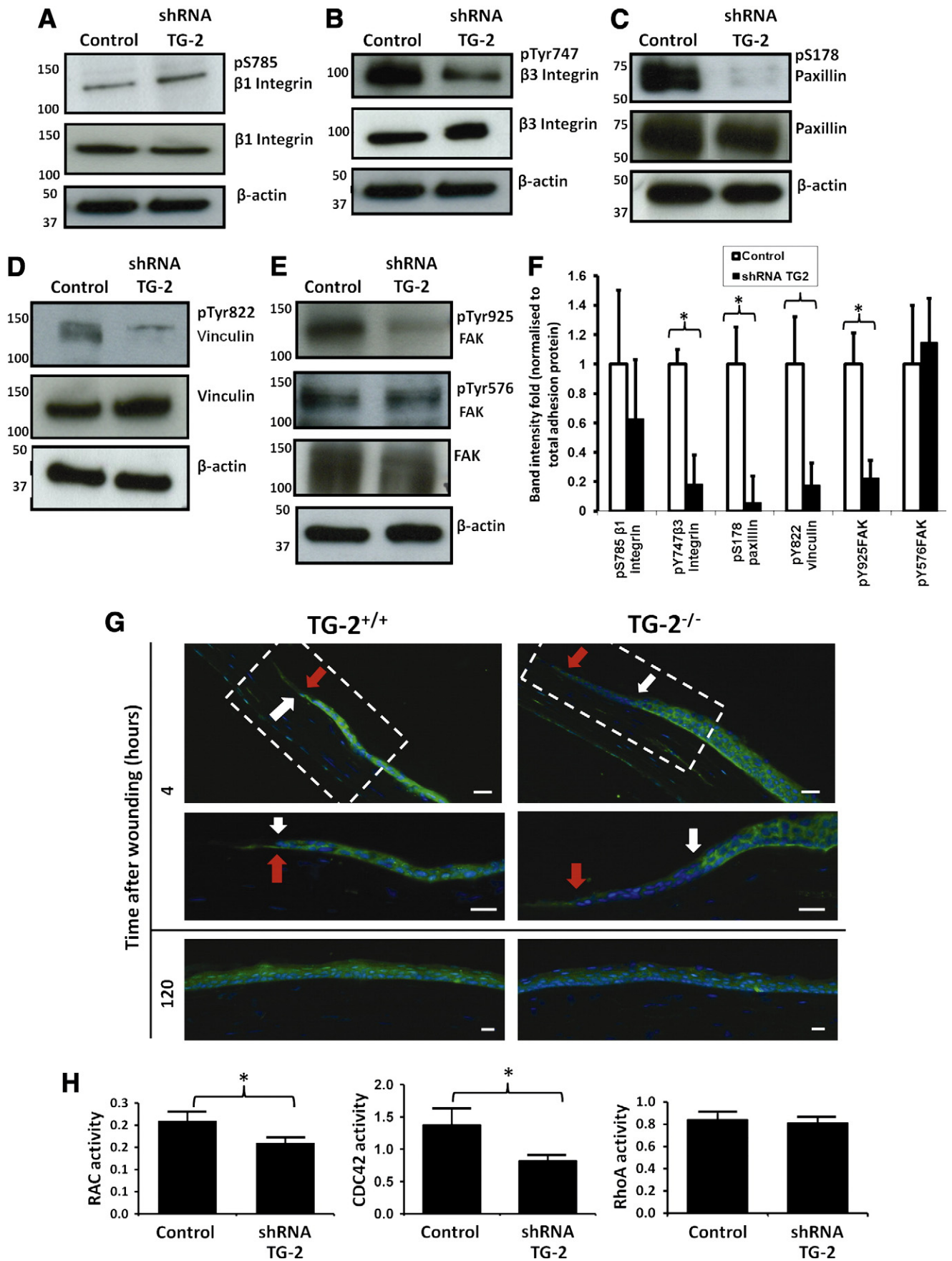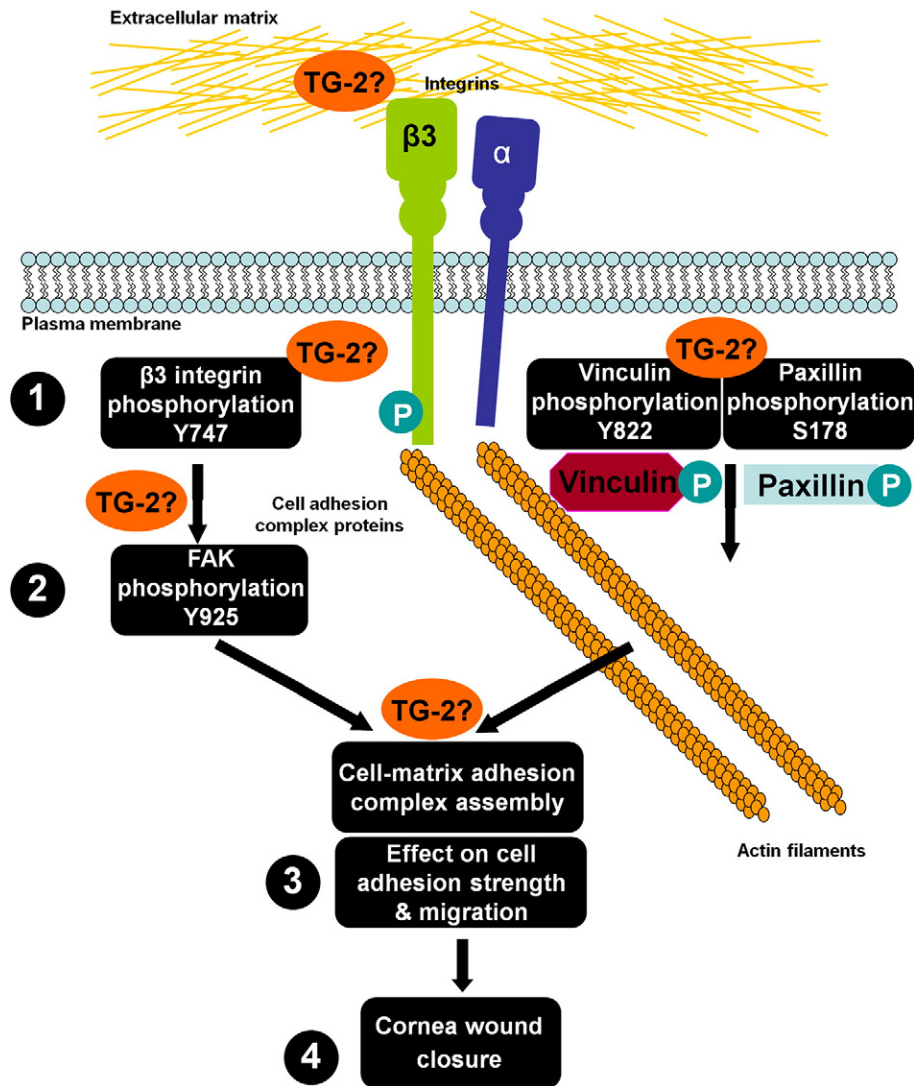
Fig. 7. Schematic showing possible sites of TG2 involvement in human corneal epithelial cell adhesion and migration. FAK: focal adhesion kinase.

enhancement of actin polymerization, in cells expressing shRNA against TG-2 we observed the disruption of the actin cytoskeleton in cells at the edge of the scratch wound (Fig. 5) and reduced activation of small GTPases, Rac and CDC42 (Fig. 6H), relative to cells expressing scrambled shRNA. It is thus tempting to speculate that TG-2 enhances corneal epithelial cell adhesion and migration through a pathway involving β-3 integrin activation and serine-phosphorylation of paxillin simultaneous with Rac and CDC42 activation.

Of interest, cell surface TG-2 has been shown to promote the activation of RhoA, upon nascent adhesion of fibroblasts, via β-1 integrin clustering and down-regulation of the Src-p190RhoGAP signaling pathway [17]. Our current report has not extended to the study of clustering of adhesion molecules. This will be evaluated in future studies.

We were not able to study the effect of over-expressing TG-2 in corneal epithelial cells because this intervention induced a significant amount of cell apoptosis and made it difficult to achieve confluence for scratch test assays (data not shown). We were also unable to consistently rescue migration by the addition of recombinant human TG2 to the media or by coating the culture vessels with recombinant human TG2. This could be due to several reasons: insufficient quantity of TG2 delivered, poor activity of the added TG2, or inappropriate cellular localization of the added TG2.

Our findings may be exploited in clinical scenarios such as neurotrophic corneal ulcers in diabetics or persistent corneal epithelial defects. Epithelial cell adhesion and migration are only one out of the many processes in corneal wound healing. Processes such as keratocyte cell death, inflammation, and myofibroblast formation are also involved [38,39]. Although TG-2 may potentially be involved in these other wound healing events [15], our work currently only focused on the corneal epithelial cell and the role of TG-2 in cell adhesion/migration.

In summary, the presence of TG-2 enhances wound healing in corneal epithelium through its effects on the phosphorylation of key cell adhesion proteins. Since serine phosphorylation of paxillin has been linked to the adhesion of not only epithelial cells but also fibroblasts [40], and TG-2 affects the adhesion of many cell types [15], serine phosphorylation of paxillin in a TG-2-dependent manner may be a conserved signal transduction mechanism for cell adhesion and cytoskeletal reorganization, and is perhaps activated in all stratified epithelium. The exact sequence of signaling events, and the interactions of TG-2 with various extra- or intracellular molecules in this pathway, remain to be determined, as does the role of TG-2 in diseases like recurrent corneal erosions, stem cell failure and corneal epitheliopathy in dry eye and infection.

References

[1] K. Mehta, J.Y. Fok, L.S. Mangala, Tissue transglutaminase: from biological glue to cell survival cues, Front. Biosci. 11 (2006) 173–185.

[2] S.E. Iismaa, G.E. Begg, R.M. Graham, Cross-linking transglutaminases with G protein-coupled receptor signaling, Sci. STKE 2006 (2006) pe34.

[3] S.E. Iismaa, B.M. Mearns, L. Lorand, R.M. Graham, Transglutaminases and disease: lessons from genetically engineered mouse models and inherited disorders, Physiol. Rev. 89 (2009) 991–1023.

[4] E. Verderio, C. Gaudry, S. Gross, C. Smith, S. Downes, M. Griffin, Regulation of cell surface tissue transglutaminase: effects on matrix storage of latent transforming growth factor-beta binding protein-1, J. Histochem. Cytochem. 47 (1999) 1417–1432.

[5] S.S. Akimov, D. Krylov, L.F. Fleischman, A.M. Belkin, Tissue transglutaminase is an integrin-binding adhesion coreceptor for fibronectin, J. Cell Biol. 148 (2000) 825–838.

[6] C. Esposito, M.L. Lombardi, V. Ruocco, A. Cozzolino, L. Mariniello, R. Porta, Implication of tissue transglutaminase and desmoplakin in cell adhesion mechanism in human epidermis, Mol. Cell. Biochem. 206 (2000) 57–65.

[7] A.M. Belkin, G. Tsurupa, E. Zemskov, Y. Veklich, J.W. Weisel, L. Medved, Transglutaminase-mediated oligomerization of the fibrin(ogen) alphaC domains promotes integrin-dependent cell adhesion and signaling, Blood 105 (2005) 3561–3568.

[8] S.S. Akimov, A.M. Belkin, Cell surface tissue transglutaminase is involved in adhesion and migration of monocytic cells on fibronectin, Blood 98 (2001) 1567–1576.

[9] L. Lorand, R.M. Graham, Transglutaminases: crosslinking enzymes with pleiotropic functions, Nat. Rev. Mol. Cell Biol. 4 (2003) 140–156.

[10] E.A. Verderio, D. Telci, A. Okoye, G. Melino, M. Griffin, A novel RGD-independent cell adhesion pathway mediated by fibronectin-bound tissue transglutaminase rescues cells from anoikis, J. Biol. Chem. 278 (2003) 42604–42614.

[11] M. Raghunath, R. Cankay, U. Kubitscheck, J.D. Fauteck, R. Mayne, D. Aeschlimann, U. Schlotzer-Schrehardt, Transglutaminase activity in the eye: cross-linking in epithelia and connective tissue structures, Invest. Ophthalmol. Vis. Sci. 40 (1999) 2780–2787.

[12] J. Sohn, T.I. Kim, Y.H. Yoon, J.Y. Kim, S.Y. Kim, Novel transglutaminase inhibitors reverse the inflammation of allergic conjunctivitis, J. Clin. Invest. 111 (2003) 121–128.

[13] Y.J. Kim, E.S. Park, K.Y. Song, S.C. Park, J.C. Kim, Glutathione transferase (class pi) and tissue transglutaminase (Tgase C) expression in pterygia, Korean J. Ophthalmol. 12 (1998) 6–13.

[14] W. Zhang, A. Shiraishi, A. Suzuki, X. Zheng, T. Kodama, Y. Ohashi, Expression and distribution of tissue transglutaminase in normal and injured rat cornea, Curr. Eye Res. 28 (2004) 37–45.

[15] E.A. Verderio, T. Johnson, M. Griffin, Tissue transglutaminase in normal and abnormal wound healing: review article, Amino Acids 26 (2004) 387–404.

[16] K. Kimura, S. Teranishi, J. Yamauchi, T. Nishida, Role of JNK-dependent serine phosphorylation of paxillin in migration of corneal epithelial cells during wound closure, Invest. Ophthalmol. Vis. Sci. 49 (2008) 125–132.

[17] A. Janiak, E.A. Zemskov, A.M. Belkin, Cell surface transglutaminase promotes RhoA activation via integrin clustering and suppression of the Src-p190RhoGAP signaling pathway, Mol. Biol. Cell 17 (2006) 1606–1619.

[18] N. Nanda, S.E. Iismaa, W.A. Owens, A. Husain, F. Mackay, R.M. Graham, Targeted inactivation of Gh/tissue transglutaminase II, J. Biol. Chem. 276 (2001) 20673–20678.

[19] K. Araki-Sasaki, Y. Ohashi, T. Sasabe, K. Hayashi, H. Watanabe, Y. Tano, H. Handa, An SV40-immortalized human corneal epithelial cell line and its characterization, Invest. Ophthalmol. Vis. Sci. 36 (1995) 614–621.

[20] E. Png, G.K. Samivelu, S.H. Yeo, J. Chew, S.S. Chaurasia, L. Tong, Hyperosmolarity mediated mitochondrial dysfunction requires transglutaminase-2 in human corneal epithelial cells, J. Cell. Physiol. 226 (2010) 693–699.

[21] I.H. Heijink, S.M. Brandenburg, J.A. Noordhoek, D.S. Postma, D.J. Slebos, A.J. van Oosterhout, Characterisation of cell adhesion in airway epithelial cell types using electric cell-substrate impedance sensing, Eur. Respir. J. 35 (2010) 894–903.

[22] A.K. Riau, T.T. Wong, R.W. Beuerman, L. Tong, Calcium-binding S100 protein expression in pterygium, Mol. Vis. 15 (2009) 335–342.

[23] M.A. Stepp, Corneal integrins and their functions, Exp. Eye Res. 83 (2006) 3–15.

[24] C. Le Clainche, M.F. Carlier, Regulation of actin assembly associated with protrusion and adhesion in cell migration, Physiol. Rev. 88 (2008) 489–513.

[25] S.G. Priglinger, C.S. Alge, A.S. Neubauer, N. Kristin, C. Hirneiss, K. Eibl, A. Kampik, U. Welge-Lussen, TGF-beta2-induced cell surface tissue transglutaminase increases adhesion and migration of RPE cells on fibronectin through the gelatin-binding domain, Invest. Ophthalmol. Vis. Sci. 45 (2004) 955–963.

[26] R.A. Jones, B. Nicholas, S. Mian, P.J. Davies, M. Griffin, Reduced expression of tissue transglutaminase in a human endothelial cell line leads to changes in cell spreading, cell adhesion and reduced polymerisation of fibronectin, J. Cell Sci. 110 (Pt 19) (1997) 2461–2472.

[27] J. Forsprecher, Z. Wang, V. Nelea, M.T. Kaartinen, Enhanced osteoblast adhesion on transglutaminase 2-crosslinked fibronectin, Amino Acids 36 (2009) 747–753.

[28] L.S. Mangala, B. Arun, A.A. Sahin, K. Mehta, Tissue transglutaminase-induced alterations in extracellular matrix inhibit tumor invasion, Mol. Cancer 4 (2005) 33.

[29] D.G. Menter, J.T. Patton, T.V. Updyke, R.S. Kerbel, M. Maamer, L.V. McIntire, G.L. Nicolson, Transglutaminase stabilizes melanoma adhesion under laminar flow, Cell Biophys. 18 (1991) 123–143.

[30] J.M. Jeong, S.N. Murthy, J.T. Radek, L. Lorand, The fibronectin-binding domain of transglutaminase, J. Biol. Chem. 270 (1995) 5654–5658.

[31] Z. Zou, H. Chen, A.A. Schmaier, R.O. Hynes, M.L. Kahn, Structure-function analysis reveals discrete beta3 integrin inside-out and outside-in signaling pathways in platelets, Blood 109 (2007) 3284–3290.

[32] D.A. Law, L. Nannizzi-Alaimo, D.R. Phillips, Outside-in integrin signal transduction. Alpha IIb beta 3-(GP IIb IIIa) tyrosine phosphorylation induced by platelet aggregation, J. Biol. Chem. 271 (1996) 10811–10815.

[33] S.D. Blystone, M.P. Williams, S.E. Slater, E.J. Brown, Requirement of integrin beta3 tyrosine 747 for beta3 tyrosine phosphorylation and regulation of alphavbeta3 avidity, J. Biol. Chem. 272 (1997) 28757–28761.

[34] C.P. Gayer, L.S. Chaturvedi, S. Wang, B. Alston, T.L. Flanigan, M.D. Basson, Delineating the signals by which repetitive deformation stimulates intestinal epithelial migration across fibronectin, Am. J. Physiol. Gastrointest. Liver Physiol. 296 (2009) G876–G885.

[35] A.J. Ridley, Rho GTPases and actin dynamics in membrane protrusions and vesicle trafficking, Trends Cell Biol. 16 (2006) 522–529.

[36] K. Kurokawa, R.E. Itoh, H. Yoshizaki, Y.O. Nakamura, M. Matsuda, Coactivation of Rac1 and Cdc42 at lamellipodia and membrane ruffles induced by epidermal growth factor, Mol. Biol. Cell 15 (2004) 1003–1010.

[37] C.D. Nobes, A. Hall, Rho, rac, and cdc42 GTPases regulate the assembly of multimolecular focal complexes associated with actin stress fibers, lamellipodia, and filopodia, Cell 81 (1995) 53–62.

[38] M.E. Fini, Keratocyte and fibroblast phenotypes in the repairing cornea, Prog. Retin. Eye Res. 18 (1999) 529–551.

[39] S.E. Wilson, M. Netto, R. Ambrosio Jr., Corneal cells: chatty in development, homeostasis, wound healing, and disease, Am. J. Ophthalmol. 136 (2003) 530–536.

[40] S.L. Bellis, J.A. Perrotta, M.S. Curtis, C.E. Turner, Adhesion of fibroblasts to fibronectin stimulates both serine and tyrosine phosphorylation of paxillin, Biochem. J. 325 (Pt 2) (1997) 375–381.